Distinct effects of conductive materials on anaerobic sulfate-rich wastewater treatment under varying operational modes

Water Research 287 (2025) 124384

Contents lists available at ScienceDirect

Water Research

journal homepage: www.elsevier.com/locate/watres

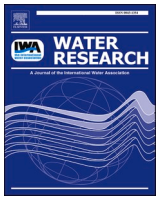

Distinct effects of conductive materials on anaerobic sulfate-rich wastewater treatment under varying operational modes

Wenhui Shu, Guangxue Wu *

Civil Engineering, School of Engineering, College of Science and Engineering, University of Galway, Galway H91 TK33, Ireland

ARTICLE INFO

Keywords:
Anaerobic digestion
Conductive materials
Direct interspecies electron transfer
Microbial syntrophic interactions
Sulfate-reducing bacteria

ABSTRACT

Conductive materials (CMs) have shown great potential in enhancing anaerobic digestion of sulfate-rich wastewater by improving electron transfer. However, how the effectiveness of CMs varies under different reactor operational modes that shape microbial communities and influence system performance remains poorly understood. This study systematically compared sequencing batch reactors (SBRs) and continuous-flow reactors (CFRs) amended with magnetite (Fe_3O_4) or powdered activated carbon (PAC) for treating sulfate-rich wastewater. CM amendments significantly accelerated sulfate reduction, volatile fatty acids degradation, and methane production, especially with the addition of Fe_3O_4. Maximum methanogenesis rates in CFRs increased from 31.2 mg COD/(g VSS·h) without CMs to 51.0 and 39.7 mg COD/(g VSS·h) with the addition of Fe_3O_4 and PAC, respectively. Methanogenesis in SBRs was severely inhibited by elevated hydrogen sulfide concentrations, and supplementation with 1 g/L CMs failed to alleviate this inhibition. CFRs favored direct ethanol-to-acetate conversion, whereas SBRs activated ethanol-to-propionate metabolic pathway mediated by *Desulfobulbus*. CM additions led to increased sludge conductivity and electron transport activity. Specifically, PAC strongly enhanced electron transfer in CFRs by promoting e-pili and cytochrome gene abundances, whereas Fe_3O_4 in SBRs predominantly acted as an external conductive conduit, partially substituting intrinsic microbial conductive structures. Key sulfate-reducing bacteria (SRB), including *Unclassified_f_Desulfovibrionaceae, Desulfomicrobium, Desulfolutivibrio*, and *Desulfovibrio*, dominated the expression of e-pili and cytochrome genes associated with the direct interspecies electron transfer, which was promoted by CFR operation through the enrichment of SRB. Microbial co-occurrence network analysis further highlighted *Desulfovibrio, Methanothrix*, and *Geobacter* as central keystone species mediating robust syntrophic electron transfer networks. These findings provide critical insights for optimizing sulfate-rich wastewater treatment through strategic selection of reactor modes and CMs.

1. Introduction

Anaerobic digestion (AD) is a cost-effective technology for treating sulfate-rich wastewater while producing bioenergy. Such wastewaters, commonly discharged from industries like pulp and paper, pharmaceuticals, and tannery, typically contain sulfate concentrations ranging from 400 to 4000 mg/L (Kibangou et al., 2022; Xie et al., 2022; Tong et al., 2023). In AD systems, sulfate-reducing bacteria (SRB) can outcompete methanogens for key intermediates such as acetate, hydrogen, and formate, due to the thermodynamic advantage of sulfate reduction (Zhang et al., 2022b). Furthermore, the produced inhibitory hydrogen sulfide (H_2S) may suppress methane yields and cause process instability (Olivera et al., 2022). Therefore, understanding and mitigating the impacts of SRB competition and H_2S inhibition are essential for improving the stability and efficiency of anaerobic sulfate-rich wastewater treatment.

The addition of conductive materials (CMs) such as iron and carbon-based materials has been found to alleviate inhibition when treating sulfate-rich wastewater using AD systems (Chen et al., 2023b; Jung et al., 2023; Xu et al., 2023). Iron-based materials such as zero-valent iron (ZVI) and magnetite (Fe_3O_4) have been shown to markedly stimulate methanogenic activity. For instance, Paepatung et al. (2022) reported that a one-time addition of 210 g ZVI revived methanogenesis in a sulfate-rich system (COD/SO_4^{2-} ratio of 2), raising CH_4 production from near-zero to 0.54 ± 0.15 L/(L·d) and enhancing hydrogenotrophic activity by over 72 times. Similarly, Fe_3O_4 supplementation up to 10 g/L led to a 30.5% increase in cumulative methane yield and a 78.5% reduction in H_2S generation by promoting sulfide oxidation to elemental

* Corresponding author.
E-mail address: guangxue.wu@universityofgalway.ie (G. Wu).

https://doi.org/10.1016/j.watres.2025.124384
Received 5 June 2025; Received in revised form 18 July 2025; Accepted 9 August 2025
Available online 10 August 2025

sulfur (S^0) (Wang et al., 2024b). Carbon-based materials such as granular activated carbon (GAC) have been shown to enhance microbial cooperation and resistance to H_2S toxicity. Chen et al. (2023a) demonstrated that GAC simultaneously stimulated the growth of *Desulfovibrio* and *Methanosaeta*, while Zhang et al. (2022a) showed that GAC promoted syntrophic associations between methanogens and specific fermentative bacteria such as *Bacteroidetes_vadinHA17* and *Trichococcus*, increasing methane production by 32-78% under H_2S stress. In another study, GAC addition resulted in 11-20% higher methane yield which was attributed to the enrichment of electroactive and hydrogenotrophic methanogens (Zhang et al., 2021).

Despite these advancements, most existing studies in sulfate-rich systems have examined the effects of CMs within either continuous-flow (e.g., up-flow anaerobic sludge blanket, continuously stirred tank reactor) (Giangeri et al., 2023; Chen et al., 2023a; Jung et al., 2020) or batch-like conditions (e.g., sequencing batch reactor (SBR), fed-batch) (Xue et al., 2024; Paepatung et al., 2022; Liu et al., 2019), with limited direct comparisons of how CMs interact with different reactor operational modes. However, operational modes can influence microbial community composition, electron transfer dynamics, and system performance by shaping substrate gradients and hydraulic regimes (Zakaria and Dhar, 2022; Simon et al., 2006). SBRs create high substrate gradients and favor fast-growing microorganisms with high substrate uptake rates (Rombouts et al., 2019). Their cost-effectiveness and high operational flexibility have made them popular in small- to medium-scale applications with intermittent or highly variable influent (Lauzurique et al., 2023). In contrast, continuous-flow reactors (CFRs) with a low substrate gradient support the development of slower-growing but more energy-efficient populations, such as the representative electroactive bacterium *Geobacter* (Du et al., 2024). This operational stability benefits large-scale applications, enabling better effluent quality, biomass retention, and energy efficiency (Wang et al., 2021). Under sulfate-rich conditions, operational modes also influence the dominance of different types of functional microorganisms, which respond divergently to H_2S stress (Shu et al., 2025b). Yet, how reactor-driven microbial selection influences the effectiveness of CMs under sulfate-reducing conditions is still poorly understood. Gaining such insights is essential for advancing the engineering application of CMs in high-sulfate anaerobic systems.

To bridge these critical gaps using AD processes treating sulfate-rich wastewater, we proposed that reactor operational modes (CFR and SBR) could enrich different types of microbial communities, and then the addition of CMs (Fe_3O_4 and powdered activated carbon (PAC)) would further induce distinct system performance and electron transfer pathways. Therefore, this study aimed to: (1) investigate the influence of operational mode and CMs amendments on anaerobic reactor performance; (2) reveal the distinct microbial metabolic pathways involved in ethanol and intermediate substrate metabolism; (3) elucidate the electron transfer mechanisms promoted by Fe_3O_4 and PAC; and (4) uncover microbial interaction patterns and their roles in sustaining electron transfer through microbial co-occurrence network analysis. The research outcomes provide comprehensive insights into optimizing sulfate-rich wastewater treatment by strategically selecting appropriate reactor configurations and adding CMs.

2. Materials and methods

2.1. Reactor setup and operation

Six lab-scale anaerobic reactors (effective volume of 5 L each) were operated at 35°C, consisting of three CFRs (CFR-Fe_3O_4, CFR-PAC, and CFR-control) and three SBRs (SBR-Fe_3O_4, SBR-PAC, and SBR-control). The inoculum was collected from lab-scale anaerobic ethanol-fed reactors. Each reactor was designed with a suspended solids (SS) concentration of 4.9 ± 0.4 g/L and a volatile suspended solids (VSS) concentration of 3.1 ± 0.2 g/L. CMs were supplemented into the designated reactors at a concentration of 1 g/L Fe_3O_4 (CFR-Fe_3O_4 and SBR-Fe_3O_4) or 1 g/L PAC (CFR-PAC and SBR-PAC). A hydraulic retention time (HRT) of 48 h was adopted in all reactors. SBRs were operated in 24 h cycles comprising 23 h of anaerobic reaction (including 2.5 L rapid feeding within 10 min), 50 min settling, and 10 min of withdrawal (2.5 L per cycle). CFRs received 2.5 L continuous inflow over 23 h, followed by the same settling and withdrawal steps as SBRs.

The synthetic wastewater contained 5000 mg COD/L of ethanol as the sole organic carbon and 2500 mg/L of sulfate (equivalent to 3698 mg/L Na_2SO_4), resulting in a COD/sulfate ratio of 2:1. The inorganic salt solution was supplemented with 191 mg/L NH_4Cl, 46 mg/L Na_2HPO_4, 200 mg/L $CaCl_2{\cdot}6H_2O$, 200 mg/L $MgCl_2$, 3000 mg/L $KHCO_3$, and 1 mL/L of a trace element solution. The trace element solution consisted of 1000 mg/L $FeCl_2{\cdot}4H_2O$, 100 mg/L $CoCl_2{\cdot}H_2O$, 200 mg/L $NiCl_2{\cdot}6H_2O$, 100 mg/L $MnCl_2{\cdot}4H_2O$, 100 mg/L $Na_2MoO_4{\cdot}2H_2O$, 100 mg/L H_3BO_3, 100 mg/L $Na_2WO_4{\cdot}2H_2O$, and 100 mg/L Na_2SeO_3.

2.2. Batch experiments

To characterize the steady-state performance of each reactor, cycle experiments were conducted in 160 mL serum bottles using 50 mL of synthetic wastewater and 50 mL of sludge suspension collected from the reactors after discharging the treated wastewater. Bottles were purged with N_2 gas and sealed with butyl rubber stoppers. Subsequently, all sealed bottles were incubated in an air shaking incubator at 35°C and 170 rpm. Time-course samples over 24 h were analyzed for ethanol, volatile fatty acids (VFAs), sulfate, methane, and sulfide.

Additional batch experiments were conducted to clarify the factors influencing propionate formation observed in SBR systems. Sludge suspension (50 mL; the same as the cycle experiment) from SBR-Fe_3O_4 at steady state was mixed with synthetic wastewater under two conditions (with or without 2500 mg/L sulfate addition). To investigate the potential influence of residual acetate, another set of sludge suspension from SBR-Fe_3O_4 was washed three times using inorganic salt solution to remove residual acetate, followed by the same sulfate/no-sulfate treatments described above. All tests were conducted at 35°C, with ethanol, VFAs, and sulfate monitored over 6 h.

2.3. Analytical methods

VFAs were analyzed using gas chromatography (8860, Agilent Technologies, USA) equipped with a flame ionization detector. Ethanol and sulfate concentrations were measured by a nutrient analyzer (Gallery Plus, Thermo Fisher Scientific, USA). pH measurements were performed using a portable pH meter (HQ40D, Hach, USA). Total dissolved sulfide (TDS) in the solution was quantified via the methylene blue method (APHA, 2005). Dissolved H_2S concentrations were calculated based on TDS and pH values using the following equation (Jin et al., 2013):

$$[H_2S] = \frac{[TDS]}{1 + \frac{K}{10^{-pH}}} \quad (1)$$

where $[H_2S]$ is the soluble H_2S concentration (mg/L), $[TDS]$ is total dissolved sulfide (mg/L), and K is the first-step ionization equilibrium constant of H_2S ($10^{-6.83}$ at 35°C).

Biogas composition was analyzed using a gas chromatograph (7890A, Agilent Technologies, USA) equipped with a thermal conductivity detector. Cumulative methane production was modeled using the modified Gompertz equation (Zwietering et al., 1990):

$$P = P_{max} exp\left\{ - exp\left[\frac{eR_{max}}{P_{max}}(\lambda - t) + 1\right]\right\} \quad (2)$$

where P is the cumulative CH_4 production (mL/L), P_{max} is the maximum CH_4 production potential (mL/L), R_{max} is the maximum CH_4 production rate (mL/(L·h)), λ is the CH_4 production lag phase (h), t is the reaction

time (h), and *e* is 2.71828.

Sludge conductivity and electron transport system (ETS) activity assays were conducted as detailed in Supplementary Text S1.

2.4. Metagenomic analysis

At steady-state operation, 10 mL of well-mixed sludge was collected from each reactor to examine the microbial community structure and their functional potential. DNA was extracted using the DNeasy PowerSoil Pro Kit (QIAGEN, Germany) following the manufacturer's protocol. For 16S rRNA gene sequencing, libraries were prepared and sequenced on the Illumina HiSeq 2500 platform (Illumina, USA). For metagenomic analysis, qualified DNA was used to construct sequencing libraries, which were then sequenced on the Illumina HiSeq 2500 platform to generate 150 bp paired-end reads. Raw reads were quality trimmed and filtered using Trimmomatic (https://github.com/usadellab/Trimmomatic/), and high-quality reads were assembled into contigs using MEGAHIT (https://github.com/voutcn/megahit/). Contigs ≥200 bp were used to predict open reading frames (ORFs) using MetaGeneMark (https://github.com/gatech-genemark/MetaGeneMark-2), and ORFs were clustered into a non-redundant gene catalog (Unigenes) using Mmseqs2 (https://github.com/soedinglab/MMseqs2/). Taxonomic annotation of Unigenes was conducted by alignment with the NCBI-NR database, and functional annotation was performed using the KEGG database via BLAST.

2.5. Statistical analysis

Statistical significance between experimental groups was evaluated using *t*-tests, performed in Microsoft Excel (2021). A *P*-value less than 0.05 was considered statistically significant.

Microbial co-occurrence network analysis was conducted to explore the ecological relationships among dominant genera. The relative abundance table at the genus level was used to calculate pairwise Spearman correlation coefficients using the "psych" package in R software (v4.4.3). The resulting adjacency matrix was imported into Gephi platform for network construction and visualization.

3. Results and discussion

3.1. System performance

3.1.1. Enhanced acetate removal and methane production under CFR and CM supplementation conditions

The performance of six reactors was examined over a 76-day period (Fig. 1). Ethanol was efficiently degraded in all reactors within the initial

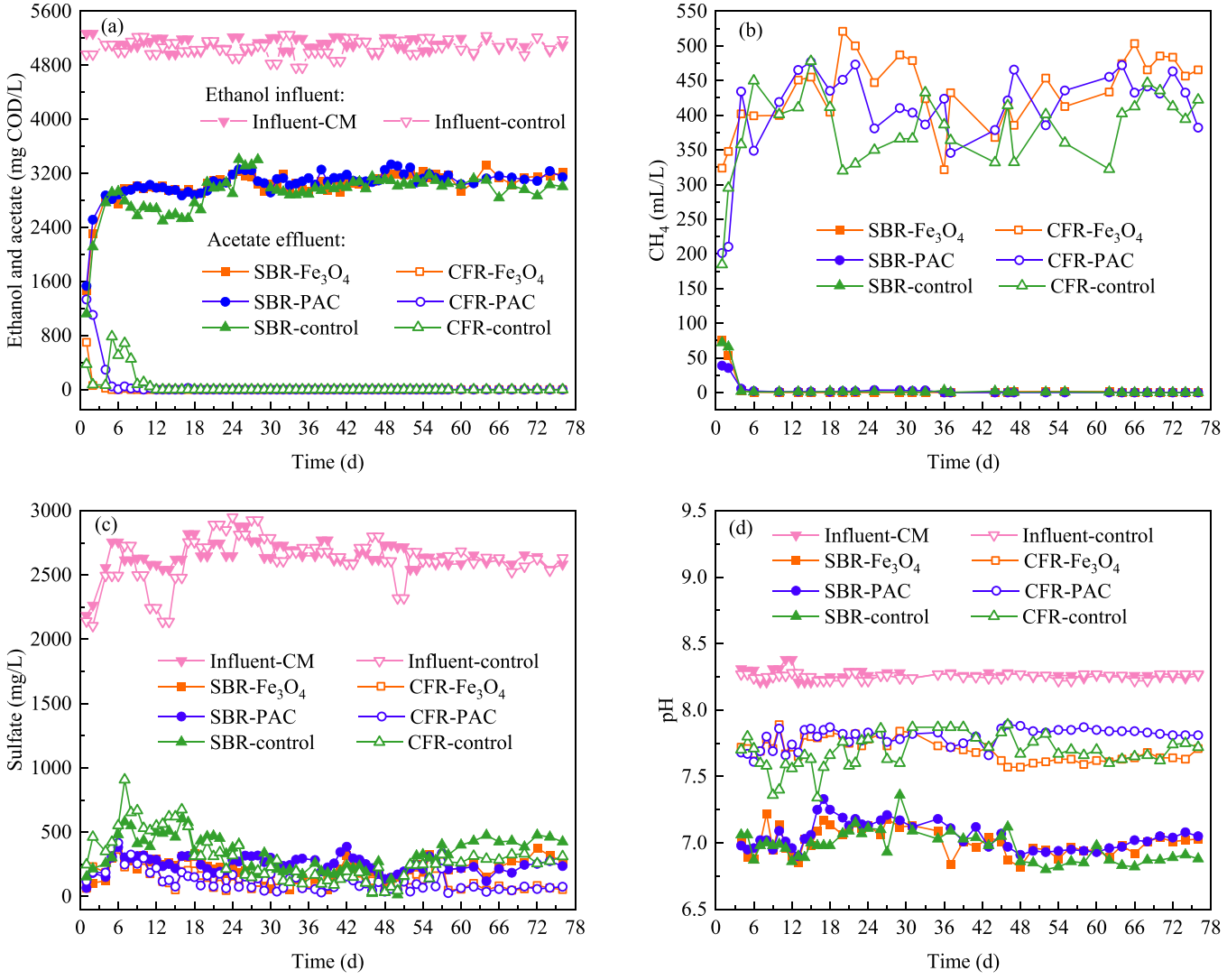

Fig. 1. Performance of six anaerobic reactors over 76 days: (a) ethanol influent and acetate effluent concentrations (effluent ethanol concentrations were below the detection limit for all reactors and thus not shown for figure clarity), (b) CH_4 production, (c) sulfate concentrations, and (d) pH values.

few days. However, distinct differences were observed in the degradation of acetate (Fig. 1a). SBRs showed a significant inhibition of downstream acetate-utilizing processes. In contrast, all CFRs exhibited complete acetate removal by day 10, with CFR-Fe_3O_4 and CFR-PAC demonstrating a rapid removal than CFR-control, suggesting that the CM addition accelerated acetate degradation.

Substantial differences in methane production were also observed (Fig. 1b). All three SBRs failed to produce detectable methane, while CFRs maintained stable methane generation. This divergence is likely due to a combination of factors. In SBRs, once-daily batch feeding may cause rapid generation and peaks of H_2S at the beginning of each cycle, leading to acute inhibition of methanogenesis. In contrast, continuous feeding in CFRs maintains a lower and more stable H_2S concentration. Additionally, although both systems operated within the generally suitable pH range for methanogenesis, SBRs had a lower pH (about 6.8-7.3) than CFRs (about 7.5-7.9) (Fig. 1d and Fig. S1). The distribution of sulfide species is strongly governed by the solution pH. Under sulfate-rich conditions, even a modest drop in pH within the common range leads to a marked increase in the unionized H_2S, which is the primary toxic form inhibiting methanogens (Lien et al., 2022; Oleszkiewicz et al.,

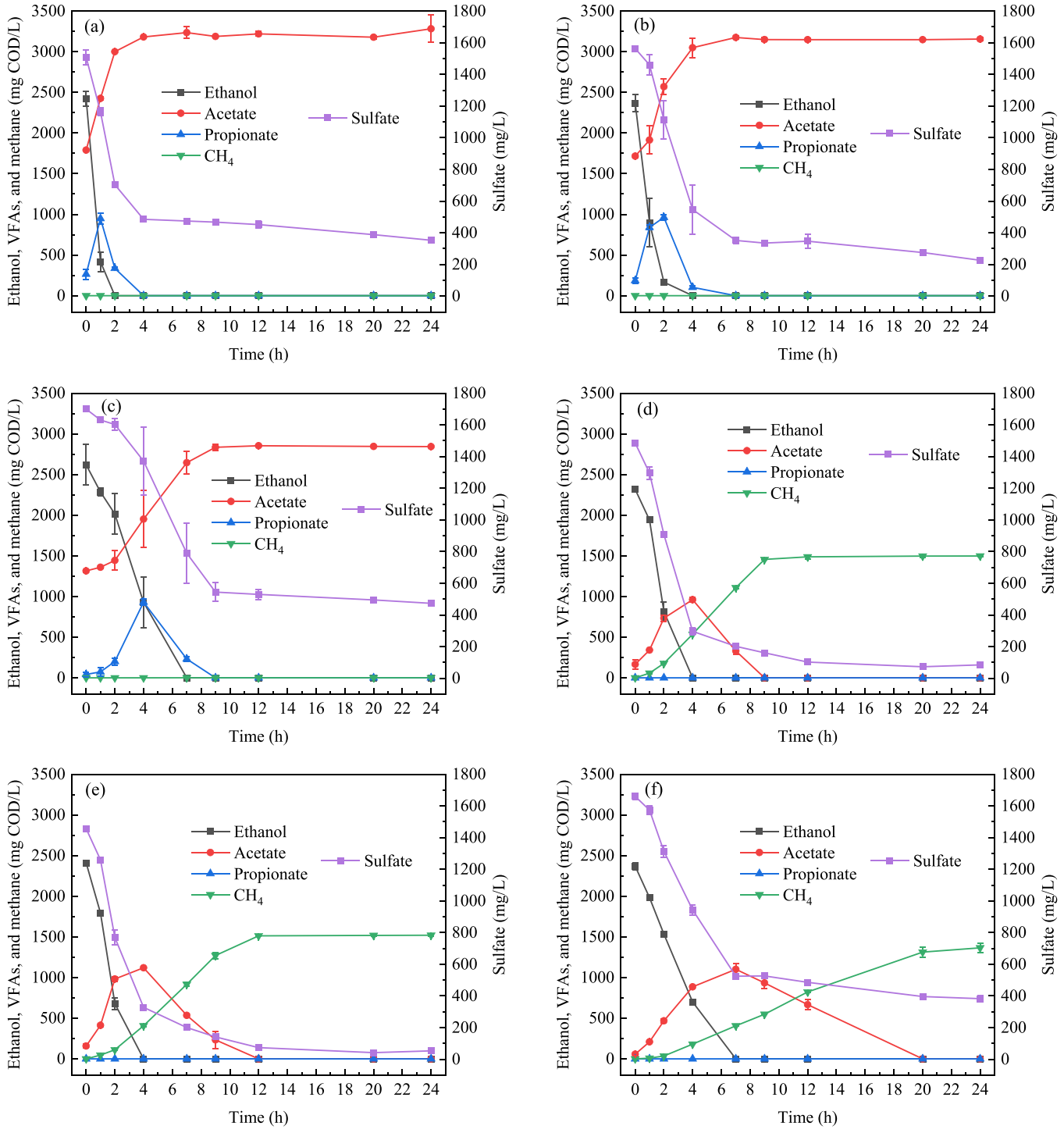

Fig. 2. Dynamics of ethanol, acetate, propionate, sulfate, and CH_4 during typical cycles in six reactors: (a) SBR-Fe_3O_4, (b) SBR-PAC, (c) SBR-control, (d) CFR-Fe_3O_4, (e) CFR-PAC, and (f) CFR-control.

1989). O'Flaherty et al. (1998) demonstrated that the toxicity of unionized H_2S is particularly pronounced for methanogens in the pH range of 6.8-7.2. Consistently, Yan et al. (2018) reported that raising the initial pH from 6.5 to 8.0 enhanced methane production by 64.1% and decreased H_2S content in biogas by 44.7%.

Sulfate reduction occurred in all reactors, yet with differing efficiencies and kinetics (Fig. 1c). Control reactors (SBR-control and CFR-control) exhibited slower sulfate reduction than their CM-amended counterparts. During the last 20 days of operation, average effluent sulfate concentrations were lower in CM-amended groups (CFR-Fe_3O_4: 95.1 ± 73.0 mg/L; CFR-PAC: 73.5 ± 48.3 mg/L; SBR-Fe_3O_4: 259.6 ± 56.8 mg/L; and SBR-PAC: 233.3 ± 53.3 mg/L) than in their respective controls (CFR-control: 291.4 ± 29.3 mg/L; SBR-control: 410.1 ± 58.7 mg/L), confirming improved sulfate reduction with the CM addition, and CFRs exhibited superior removal. Therefore, the addition of Fe_3O_4 or PAC enhanced both sulfate reduction and acetate conversion.

3.1.2. Operational mode and CMs drive divergent VFA metabolism and methanogenesis under H_2S stress

Cycle experiments were conducted to evaluate ethanol, VFAs, methane, and sulfate metabolic dynamics (Fig. 2). Ethanol was completely degraded within 7 hours in all reactors, with CM-amended groups exhibiting faster ethanol removal than their respective controls. Notably, ethanol was primarily converted to both acetate and propionate in SBRs (Fig. 2a–c), while conversion occurred predominantly to acetate in CFRs (Fig. 2d–f), indicating distinct metabolic pathway preferences shaped by reactor configurations. This divergence may be attributed to differences in substrate gradients, metabolite accumulation, electron acceptor availability, and the selective enrichment of functional microorganisms shaped by operational modes. Similar findings have been reported, highlighting that reactor configurations play a key role in steering VFA metabolic pathways even under sulfate-free conditions (Du et al., 2024; Du et al., 2023). The degradation rates of propionate in SBR-Fe_3O_4, SBR-PAC, and SBR-control were 109.3, 61.8, and 45.2 mg COD/(g VSS·h), respectively. This demonstrated that both CMs enhanced propionate degradation, with Fe_3O_4 showing a stronger effect (Cruz Viggi et al., 2014). Liu et al. (2019) and Giangeri et al. (2023) both found that Fe_3O_4 addition effectively prevented the accumulation of both acetate and propionate in sulfate-reducing anaerobic systems, supporting the role of Fe_3O_4 in facilitating syntrophic VFA oxidation. In contrast, CFRs showed no propionate accumulation, and CM addition benefited acetate removal.

Enhanced VFAs degradation was consistently associated with higher methane production in CFRs, whereas CH_4 generation remained negligible in all SBRs. R_{max} in CFR-Fe_3O_4, CFR-PAC, and CFR-control were 51.0, 39.7, and 31.2 mg COD/(g VSS·h), respectively. Fe_3O_4 and PAC addition primarily reflected in enhanced R_{max} and shortened lag phases in CFRs, while showing limited effect on cumulative CH_4 yield. Similar findings were also obtained under sulfate-rich conditions (Liang et al., 2025; Liu et al., 2019). Literature reports vary, with some noting improved CH_4 production upon GAC or Fe_3O_4 addition (Wang et al., 2024a and 2024b). This divergence may reflect differences in reactor configurations or the severity of sulfide inhibition. Moreover, unionized H_2S concentrations were notably higher in SBRs (233.1 ± 9.8 mg/L) than in CFRs (101.5 ± 8.9 mg/L) (Fig. S2). According to Shu et al. (2025b), acetoclastic methanogens exhibit 50% inhibition at H_2S concentrations ranging from 62.1 to 113.2 mg/L under comparable conditions. Given that the H_2S levels in SBRs exceeded this inhibitory threshold by a wide margin, the severe suppression of methanogenesis observed in SBRs could be reasonably attributed to H_2S toxicity. In this study, CMs were applied at a dosage of 1 g/L, which did not mitigate H_2S accumulation in SBRs. Previous lab-scale studies in sulfate-rich systems typically used much higher dosages (10-20 g/L) to achieve effective H_2S mitigation and performance improvement (Wang et al., 2024b; Zhang et al., 2022a). The one-time applied dosage was substantially low, which may be practical for full-scale applications considering cost and operational suitability. Future studies should refine dosing strategies and develop more economical, recyclable CMs.

Sulfate reduction patterns also differed across reactor configurations. With ethanol or propionate as the electron donors, sulfate removal was enhanced by CM addition in both reactor configurations. Sulfate removal rates in SBR-Fe_3O_4, SBR-PAC, and SBR-control were 108.8, 57.7, and 40.0 mg/(g VSS·h), while CFR-Fe_3O_4, CFR-PAC, and CFR-control exhibited rates of 63.8, 65.4, and 56.6 mg/(g VSS·h), respectively. The highest rate was observed in SBR-Fe_3O_4, highlighting the superior impact of Fe_3O_4 in SBRs. In contrast, sulfate reduction with acetate as the electron donor was more efficient in CFRs than SBRs, regardless of CM presence. Using acetate, sulfate removal rates were 1.8, 1.6, and 1.4 mg/(g VSS·h) in SBR-Fe_3O_4, SBR-PAC, and SBR-control, compared to 5.7, 7.2, and 3.5 mg/(g VSS·h) in CFR-Fe_3O_4, CFR-PAC, and CFR-control. These results suggest that Fe_3O_4 is more effective at promoting ethanol-mediated sulfate reduction in SBRs, while PAC provides more balanced enhancement across both ethanol- and acetate-mediated sulfate reduction in CFRs. Notably, the simultaneous enhancement of ethanol, VFAs, and sulfate degradation in CM-amended groups raises the possibility that CMs may support broader syntrophic interactions that benefit both methanogens and SRB. This observation aligns with recent hypotheses suggesting the involvement of SRB in interspecies electron exchange processes with syntrophic partners (Giangeri et al., 2023; Hu et al., 2019; Zhang et al., 2021).

3.1.3. Operational mode governs activation of the ethanol-to-propionate pathway

To elucidate the drivers of the ethanol-to-propionate (ETP) pathway in SBRs, batch assays were conducted using sludge from SBR-Fe_3O_4, evaluating the effects of sulfate and initial acetate concentrations. When unwashed sludge was used (Fig. 3a and 3b), ethanol conversion to acetate and propionate occurred under both sulfate-present and sulfate-absent conditions. Interestingly, propionate remained undegraded in the absence of sulfate, confirming that propionate oxidation is coupled to sulfate reduction. After washing to remove residual acetate (Fig. 3c and 3d), propionate formation still occurred in both the presence and absence of sulfate, suggesting that neither sulfate nor pre-existing acetate is essential for triggering the ETP pathway. Moreover, the only observed propionate degradation under sulfate presence conditions further emphasized the role of sulfate as a terminal electron acceptor in propionate oxidation. Qiao et al. (2016) demonstrated that propionate degradation often constitutes a bottleneck in AD, and the presence of sulfate can facilitate its utilization by supporting energetically favorable pathways. These results collectively indicate that the activation of the ETP route is not dictated by sulfate presence or acetate concentration but is instead shaped by the reactor configuration.

3.2. Microbial community structure

The microbial community structures diverged across the six reactors, shaped by both operational mode and CM supplementation (Fig. 4). At the phylum level (Fig. 4a), *Proteobacteria* and *Euryarchaeota* dominated the communities but exhibited distinct distributions across treatments. *Proteobacteria*, encompassing many sulfate-reducing and electroactive bacteria (Zhang et al., 2024), dominated in SBRs, especially with CM addition. In contrast, *Euryarchaeota*, primarily comprising methanogens, was more prevalent in CFRs, consistent with enhanced methanogenesis observed in these systems.

Genus-level analysis further clarified community distinctions (Fig. 4b). *Desulfobulbus* was significantly enriched in SBRs (16.2%-23.3%) compared to CFRs (<1%). As *Desulfobulbus* mediates ETP conversion and propionate oxidation (Zeng et al., 2019), its dominance in SBRs supports the prevalence of the ETP metabolic pathway under batch mode. Compared to SBRs, CFRs supported higher abundances of genera *Desulfomicrobium* and *Desulfolutivibrio*, which specialize in ethanol-to-acetate conversion, benefiting from continuous substrate

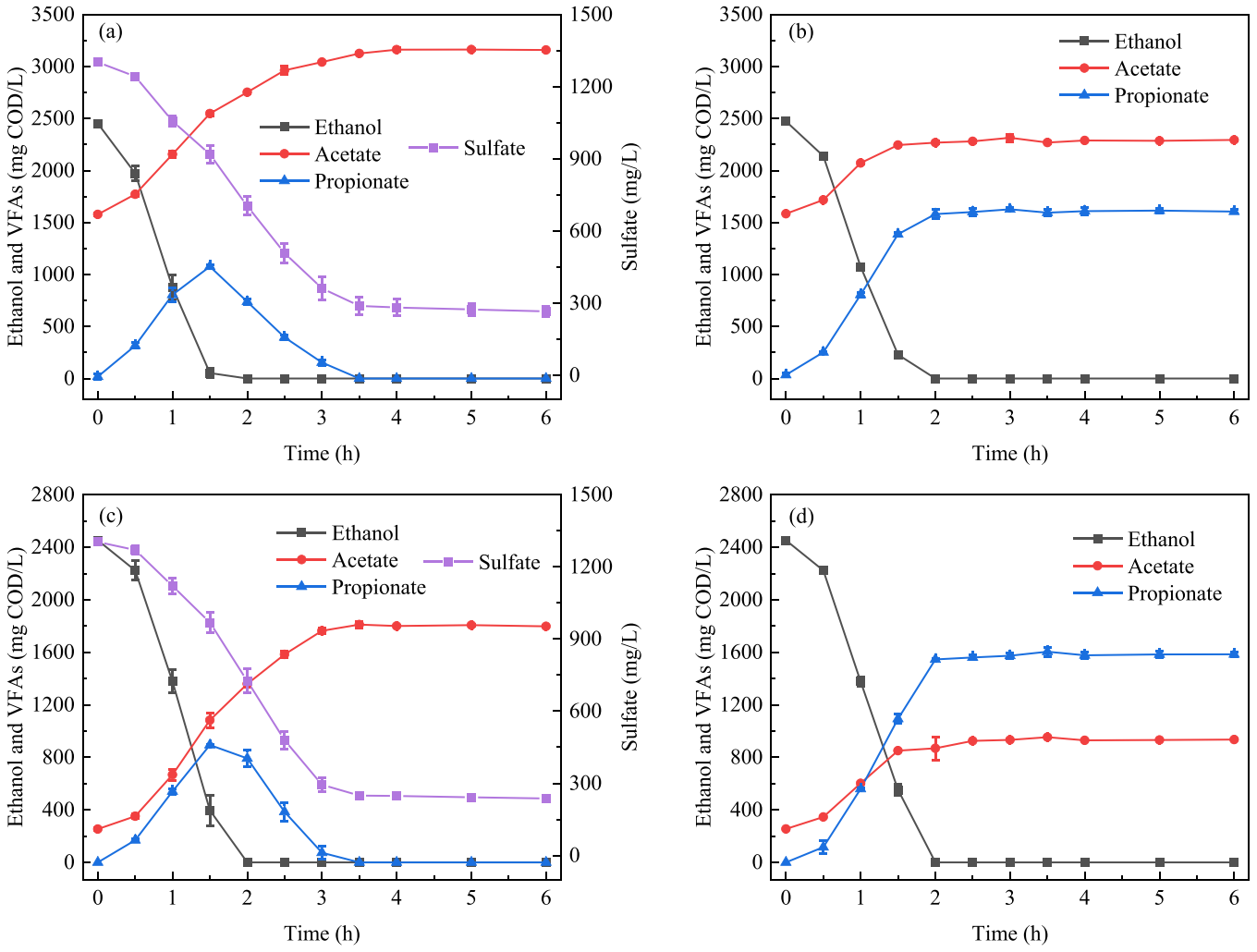

Fig. 3. Dynamics of ethanol, acetate, propionate, and sulfate during ethanol conversion under different conditions: (a) unwashed sludge with sulfate, (b) unwashed sludge without sulfate, (c) washed sludge with sulfate, and (d) washed sludge without sulfate.

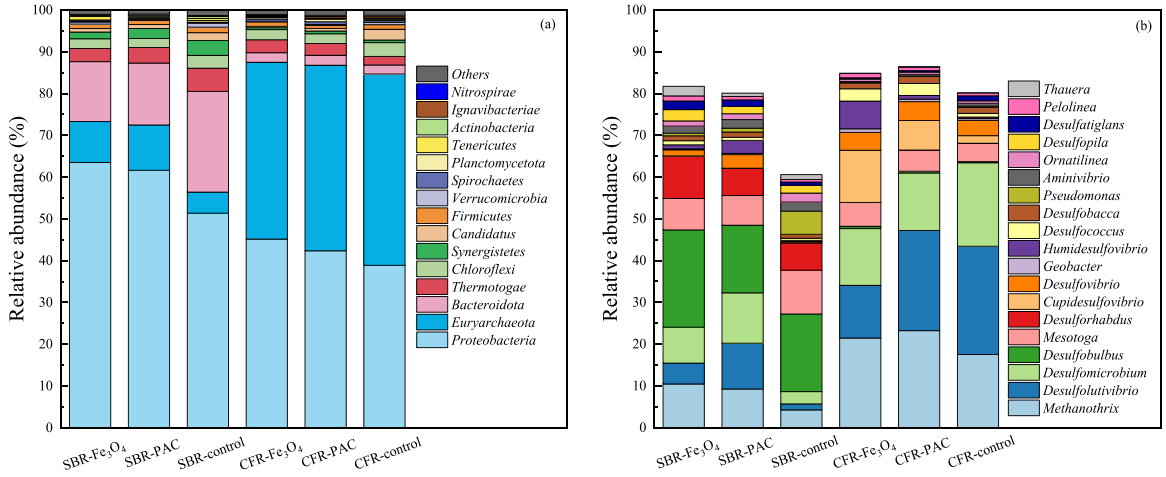

Fig. 4. Microbial community structure at the phylum level (a) and the genus level (b).

availability (Shu et al., 2025b). Interestingly, CMs addition decreased their abundances in CFRs but increased in SBRs, suggesting distinct ecological interactions or potential competition with other microorganisms such as *Methanothrix* or other SRB under varying operational modes. *Desulfovibrio* also exhibited higher relative abundances in CFRs (4.3-4.5%) than in SBRs (1.5-3.3%). Fe_3O_4 and PAC supplementation promoted the proliferation of *Desulfovibrio* in both SBR and CFR. Members of this genus are known for their metabolic flexibility, such as engaging in hydrogenotrophic sulfate reduction, as well as possessing electroactive capabilities that may contribute to electron transfer under

syntrophic conditions (Zheng et al., 2021). Additionally, *Cupidesulfovibrio*, a recently delineated genus phylogenetically separated from *Desulfovibrio* (Wan et al., 2021), showed substantial enrichment in CFRs with CMs. Its preferential enrichment under these conditions suggests a possible niche adaptation to stable electron acceptor availability and potentially enhanced extracellular electron transfer (EET), although the specific mechanisms remain to be elucidated.

Furthermore, genera *Desulfococcus* and *Desulfobacca*, responsible for acetate-coupled sulfate reduction (Oude Elferink et al., 1999; Xing et al., 2020), also exhibited higher relative abundances in CFRs. Specifically, *Desulfococcus* reached 2.94% in CFR-Fe_3O_4 and 2.86% in CFR-PAC, substantially higher than in SBRs (<1%). Similarly, *Desulfobacca* was more abundant in CFRs (1.4-1.7%) than in SBRs (0.94-1.3%). These results suggest that continuous-flow operation fosters a more favorable environment for acetate-utilizing sulfate reducers. This is likely due to their relatively lower half-saturation constant (K_S), which enables them to be enriched under low and stable acetate conditions (Shu et al., 2025a). The supplementation of CMs further promoted their relative abundances, potentially supporting syntrophic acetate oxidation or improving electron transfer efficiency during sulfate metabolism.

Geobacter, a representative electroactive genus known for its role in direct interspecies electron transfer (DIET) (Rotaru et al., 2014a), displayed relatively low but notable variations in relative abundances across reactor conditions. In CFRs, *Geobacter* exhibited higher relative abundances (0.43-0.86%) compared to SBRs (0.16-0.28%), highlighting its preference for continuous operational modes. Moreover, its abundance was consistently elevated in CM-amended groups compared to controls, particularly in CFR-Fe_3O_4 (0.86%) and CFR-PAC (0.58%), indicating Fe_3O_4 or PAC promoted *Geobacter* enrichment (Lee et al., 2020).

In parallel, *Methanothrix* was the dominant methanogen in all reactors, with its relative abundance significantly higher in CFRs (17.5-23.2%) than in SBRs (4.2-10.5%). This genus is recognized as a key acetoclastic methanogen and a DIET-associated methanogen (Rotaru et al., 2014b; Zhou et al., 2023). The pronounced enrichment of *Methanothrix* in CM-supplemented CFRs strongly supports the potential occurrence of DIET-facilitated methanogenesis in these systems. The sustained presence of *Methanothrix* in SBRs despite the absence of methane production may be attributed to their survival strategies under harsh environments. Previous studies have proposed that microorganisms may enter dormancy in response to environmental stress, stopping growth and exhibiting minimal metabolic activity while surviving a long time (McDonald et al., 2024; Xu et al., 2020). Chen et al. (2022) further demonstrated that methanogens in anaerobic granular sludge can

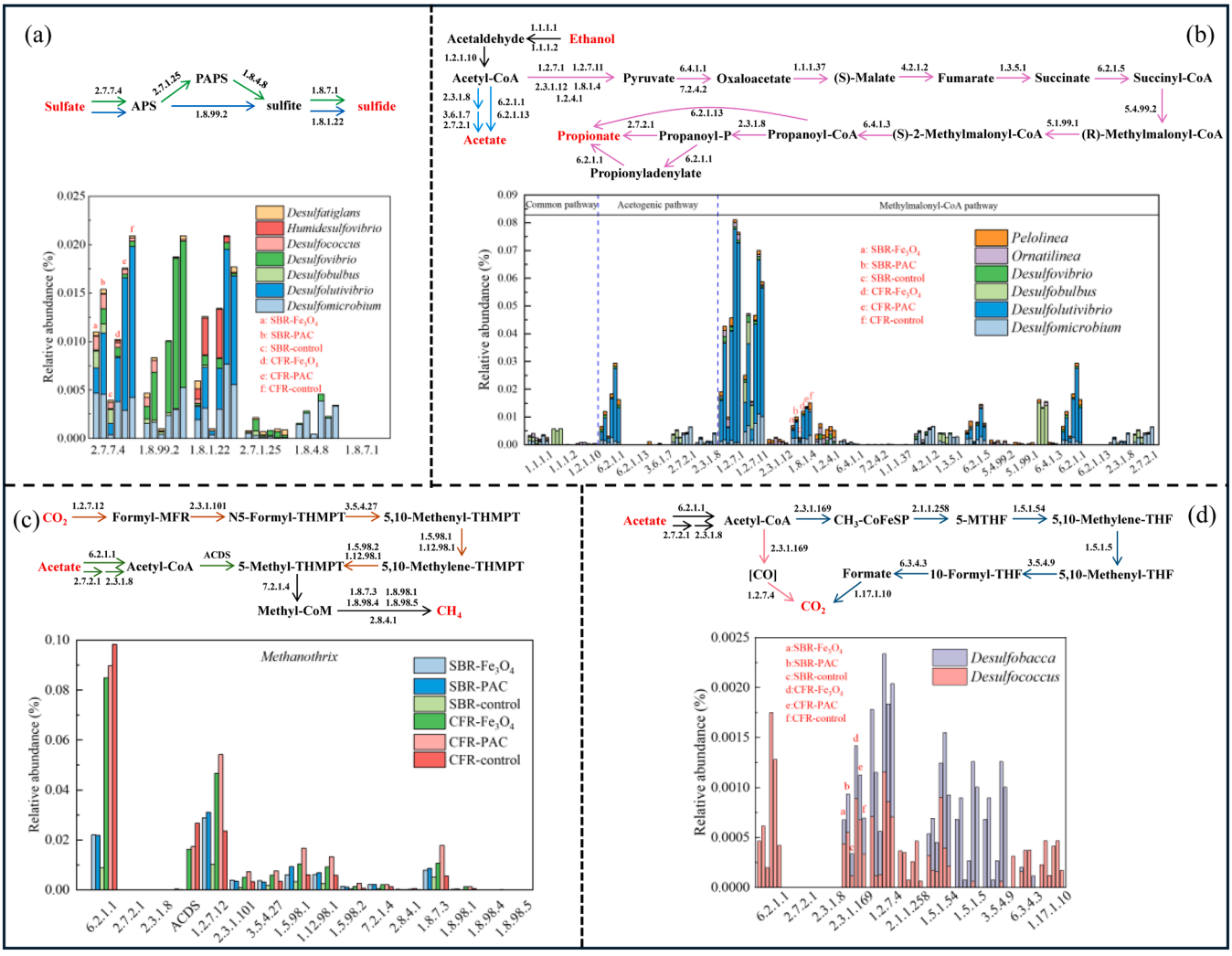

Fig. 5. Sulfate, ethanol, propionate, and acetate metabolic pathway and the relative abundances of functional enzymes encoded by key microbial involved in these processes. (a) Sulfate metabolism includes dissimilatory sulfate reduction (DSR) and assimilatory sulfate reduction (ASR) pathways. (b) Ethanol metabolism comprises ethanol to acetate and ethanol to propionate pathways, with propionate degradation following the reverse direction of methylmalonyl-CoA pathway. (c) Methane production involves acetoclastic and hydrogenotrophic methanogenesis pathways. (d) Acetate degradation proceeds via the carbon monoxide dehydrogenase pathway and the Wood-Ljungdahl pathway.

survive long-term substrate deprivation (up to 156 days) by entering a dormant state, resulting in the loss of activity while maintaining a relatively stable community structure. Therefore, the presence of *Methanothrix* in SBRs likely reflects a dormant state sustained under prolonged H_2S inhibitory conditions rather than active methanogenesis.

3.3. Metagenomic analysis

3.3.1. Sulfate metabolism and limited sulfide oxidation

Metagenomic evidence revealed that dissimilatory sulfate reduction (DSR) predominated over assimilatory sulfate reduction (ASR) in all reactors (Fig. 5a), indicating that sulfate reduction in these systems primarily served as energy metabolism (Qian et al., 2019). Among DSR genes, sulfate adenylyltransferase (EC 2.7.7.4), which initiates sulfate activation to adenosine 5′-phosphosulfate (APS), exhibited the highest relative abundance, especially in CFR-control, with major contributions from *Desulfomicrobium* and *Desulfolutivibrio*. The subsequent reduction of APS to sulfite, catalyzed by adenylyl-sulfate reductase (EC 1.8.99.2), was enriched in both SBRs and CFRs, with key contributions from *Desulfovibrio* and *Desulfomicrobium*. Notably, CM supplementation altered the terminal step of DSR (dissimilatory sulfite reductase; EC 1.8.1.22), which reduces sulfite to sulfide; a higher relative abundance was observed in CFR-PAC, suggesting that the continuous supply of electron donors and sulfate, in combination with PAC addition, promoted terminal sulfate reduction. Interestingly, while CM supplementation in CFRs did not consistently increase the gene abundance of upstream DSR genes, it led to markedly higher sulfate removal rates, indicating a disconnection between gene abundance and functional performance. This discrepancy likely arises from improved EET and metabolic efficiency enabled by Fe_3O_4 and PAC. In contrast, both Fe_3O_4 and PAC increased the gene abundance of all three DSR enzymes relative to SBR-control. This gene-level enhancement aligns with the observed increases in sulfate reduction rates in CM-amended SBRs, suggesting that under SBR conditions, gene enrichment plays a more prominent role in functional enhancement. For ASR, genes were found at much lower abundances across all reactors, reinforcing that sulfur metabolism under the studied conditions was primarily dissimilatory.

In addition to sulfate reduction, the potential for oxidizing sulfide to sulfur was assessed by examining the abundance of sulfur-oxidizing genes, including sulfide quinone reductase (*sqr*) and flavocytochrome c sulfidedehydrogenase (*fccB*). Overall, these genes exhibited low abundance across all treatments (Fig. S3), indicating that sulfur oxidation was likely a minor detoxification route under anaerobic conditions. Notably, *sqr* abundance decreased in SBR-Fe_3O_4 (0.0042%) compared to SBR-control (0.0086%), suggesting that Fe_3O_4 did not promote sulfide oxidation in batch systems. This result contrasts with the findings of Wang et al. (2024b), who reported increased functional genes abundance and effective mitigation of H_2S suppression via Fe_3O_4 supplementation in fed-batch conditions. The discrepancy may stem from differences in Fe_3O_4 dosage or microbial community composition. In contrast, *sqr* abundance increased in CFRs upon CM addition, particularly in CFR-Fe_3O_4, implying a possible material-induced stimulation of microbial sulfur oxidation under continuous feeding operation. However, *fccB* abundance remained consistently low and often declined following CM addition, further suggesting that biological sulfide oxidation likely played a limited role in mitigating sulfide accumulation in this study.

3.3.2. Microbial pathways and regulatory factors shaping ethanol and its intermediates metabolism

Ethanol metabolism proceeds through multiple intermediate steps, with carbon being ultimately converted into methane or carbon dioxide. The degradation routes diverge into two main directions: oxidation to acetate or propionate, followed by further conversion through methanogenesis or sulfate reduction. Reactor configuration and CM addition significantly influenced each stage of the process (Fig. 5b–d).

Ethanol metabolism initiated with common oxidation steps, catalyzed by alcohol dehydrogenases (EC 1.1.1.1, EC 1.1.1.2) and aldehyde dehydrogenase (EC 1.2.1.10). Subsequently, ethanol can be metabolized into either acetate or propionate. The acetogenic pathway, catalyzed by acetyl-CoA synthetase (EC 6.2.1.1), acetate kinase (EC 2.7.2.1), and phosphate acetyltransferase (EC 2.3.1.8) was more enriched in CFRs, particularly in CFR-Fe_3O_4 and CFR-PAC, with *Desulfomicrobium* and *Desulfolutivibrio* as dominant contributors. This corresponds well with the observed system performance, where ethanol was fully converted to acetate and subsequently degraded in CFRs.

Genes associated with the methylmalonyl-CoA pathway responsible for propionate formation from ethanol, such as pyruvate synthase (EC 1.2.7.1), 2-oxoacid oxidoreductase (EC 1.2.7.11), and fumarate hydratase (EC 4.2.1.2), were broadly distributed and often more abundant in CFRs. However, the key carboxylation step catalyzed by propionyl-CoA carboxylase (EC 6.4.1.3) was exclusively expressed in SBRs, particularly assigned to *Desulfobulbus* (Stams et al., 1984). This indicates that the complete pathway required for ETP conversion was only active in SBRs, which is consistent with the observed accumulation of propionate under batch conditions.

Following its formation, propionate was further metabolized via the reverse direction of the methylmalonyl-CoA pathway, converting to intermediates such as succinyl-CoA and acetate. These key degradation enzymes were predominantly attributed to *Desulfolutivibrio, Desulfomicrobium*, and notably, *Desulfobulbus*. Among these, *Desulfobulbus* played a dual role, functioning in both propionate production and oxidation. Literature reports suggest that *Desulfobulbus* is capable of fermentative ethanol-to-propionate conversion, while its ability to oxidize propionate is dependent on the presence of sulfate (Suzuki et al., 2007; El Houari et al., 2017). These observations not only highlight *Desulfobulbus* as a conditionally flexible player in SBRs, but also emphasize that propionate metabolism remained tightly coupled to sulfate availability.

Methanogenic pathways identified were mainly associated with *Methanothrix*, involving both acetoclastic and CO_2-reducing pathways. Genes encoding EC 6.2.1.1 and the acetyl-CoA decarbonylase/synthase (ACDS) complex were mainly enriched in CFRs, supporting more active acetate conversion. However, these genes showed lower abundances in CFR-Fe_3O_4 and CFR-PAC than in CFR-control, suggesting that CMs supplementation did not further enhance acetoclastic methanogenesis. In addition, CO_2-reducing pathway genes, including formylmethanofuran dehydrogenase (EC 1.2.7.12) and formyltransferase (EC 2.3.1.101), exhibited higher abundances in CFRs and CM groups, particularly in CFR-PAC. This indicates that *Methanothrix* in CFRs may perform CO_2-reducing methanogenesis via DIET, bypassing the need for hydrogen gas as an electron carrier (Rotaru et al., 2014b).

Furthermore, *Desulfobacca* and *Desulfococcus* expressed enzymes related to acetate oxidation via the carbon monoxide dehydrogenase and Wood-Ljungdahl pathways (Goevert and Conrad, 2008; Svetlitchnaia et al., 2006). While their gene contributions were relatively minor compared to methanogens, CMs supplementation increased the relative abundance of these genes, suggesting that CMs might stimulate SRB-mediated acetate degradation, possibly through enhanced EET or syntrophic interactions.

3.4. Microbial electron transfer capacity

To characterize changes in microbial electron transfer potential under CM amendment conditions, sludge conductivity, INT-ETS activity, and the predicted abundance of key genes involved in DIET were comprehensively assessed (Fig. 6).

The addition of CMs significantly enhanced sludge conductivity in both reactor configurations (Fig. 6a). The highest conductivity was recorded in SBR-Fe_3O_4 (5.1 μS/cm), representing a 1.73-fold increase compared to SBR-control. Similarly, CFR-Fe_3O_4 exhibited a 1.38-fold enhancement relative to CFR-control. PAC supplementation also substantially increased conductivity, albeit slightly lower than Fe_3O_4

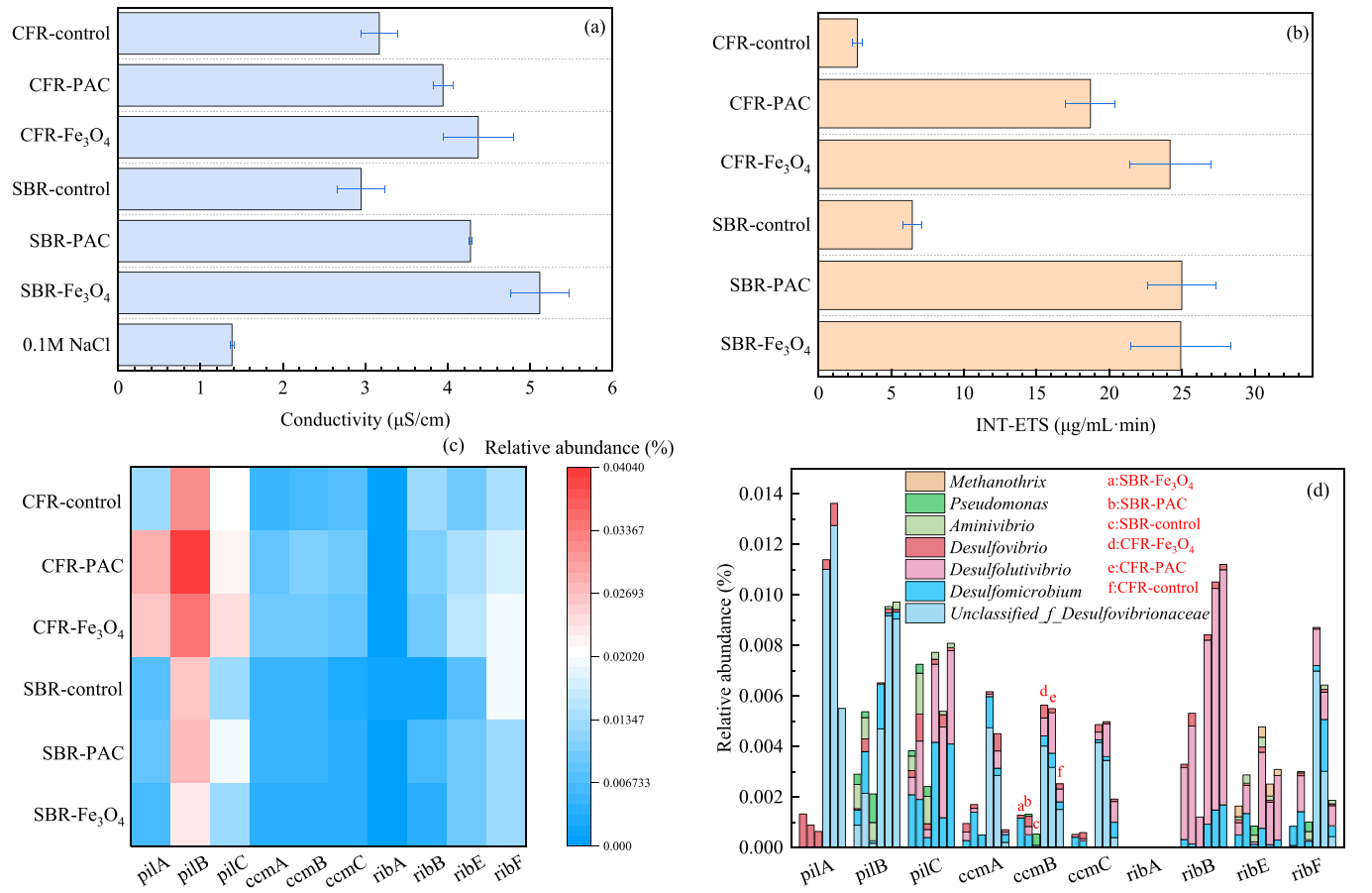

Fig. 6. Effects of conductive materials and operational mode on microbial electron transfer performance: (a) sludge conductivity; (b) INT-ETS activity; (c) relative abundances of DIET-related functional genes, including e-pili biosynthesis (*pilA, pilB, pilC*), cytochrome c biosynthesis (*ccmA, ccmB, ccmC*), and flavin biosynthesis (*ribA, ribB, ribE, ribF*); and (d) genus-level taxonomic origins of DIET-related genes.

($P < 0.05$). In parallel with conductivity enhancement, microbial ETS activity, indicative of overall respiration potential, was substantially increased in CM-amended reactors (Fig. 6b). INT reduction assays revealed that Fe_3O_4 and PAC elevated ETS activity by 3.5-4.1 times in SBRs, and approximately 2-fold in CFRs, compared to their respective controls. The strongest stimulation was observed in SBR-Fe_3O_4, suggesting that CMs not only promoted EET but also enhanced intracellular metabolic activity.

To clarify the mechanisms by which CMs and reactor configurations influence microbial electron transfer capacities, the abundances of key functional genes related to DIET were comprehensively analyzed (Fig. 6c). These genes primarily encode electrically conductive pili (e-pili: *pilA, pilB*, and *pilC*) and *c*-type cytochromes (cytochrome *c* biosynthesis genes: *ccmA, ccmB, ccmC*), which are central to DIET pathways and typically function synergistically in microbial consortia (Cavalcante et al., 2021; Giangeri et al., 2023). In CFRs, CM amendments, particularly PAC, significantly enhanced the abundance of both e-pili and cytochrome-related genes compared to the control. CFR-PAC exhibited the highest abundances of *pilA* (0.0286%), *pilB* (0.0404%), *ccmB* (0.0107%), and *ccmC* (0.0091%), clearly surpassing levels in CFR-Fe_3O_4 and CFR-control. These findings align well with PAC's known porous and conductive structure, likely facilitating microbial aggregation, physical proximity, and the establishment of robust DIET networks via both pili-mediated and cytochrome-based pathways (Zhang et al., 2023). CFR-Fe_3O_4 also promoted the relative abundance of these genes compared to the control, though the magnitude of enhancement was generally lower than PAC amendment, indicating a moderate yet consistent effect of Fe_3O_4 on DIET enhancement. Contrastingly, the gene abundance patterns showed distinct responses to different CMs in SBRs. PAC supplementation generally promoted the abundance of e-pili and cytochrome genes compared to the SBR control. However, Fe_3O_4 amendment led to reduced abundances of *pilA* (0.0065% vs. control 0.0071%) and *pilB* (0.0230% vs. control 0.0264%), despite slightly increasing *pilC* abundance. Similar trends were observed for cytochrome genes, with Fe_3O_4 supplementation resulting in either decreased or stable gene abundances compared to controls. Intriguingly, despite the lower abundance of these DIET-associated genes in SBR-Fe_3O_4, this reactor exhibited the highest sludge conductivity and INT-ETS activity. This discrepancy suggests that Fe_3O_4 may function as an external conductive conduit, compensating or partially substituting the role of intrinsic microbial conductive structures such as pili and cytochromes. Such an interpretation aligns well with previous studies reporting that CMs like magnetite can reduce microbial reliance on endogenous electron transfer pathways by acting as extracellular electron conduits, thereby downregulating the expression of DIET-related structures under certain conditions (Liu et al., 2015; Zheng et al., 2018; Jin et al., 2019).

Additional potential DIET pathways about soluble redox mediators, such as flavins, were also assessed (Zeng et al., 2024). Riboflavin biosynthesis genes (*ribB, ribE, ribF*) exhibited relatively higher abundances, particularly in CFR conditions. Notably, *ribF* showed pronounced enrichment in CFR-Fe_3O_4 (0.0201%) and CFR-PAC (0.0169%) relative to SBR groups, suggesting flavin-mediated electron shuttling may act as a complementary mechanism enhancing microbial electron transfer under continuous feeding conditions.

To identify the functional contributors of DIET-related gene expression, the taxonomic origins of key electron transfer genes were resolved at the genus level (Fig. 6d). Several dominant SRB genera, including *Unclassified_f_Desulfovibrionaceae, Desulfomicrobium, Desulfolutivibrio*,

and *Desulfovibrio* emerged as primary contributors to e-pili, cytochrome, and flavin biosynthesis genes, reflecting their central roles in DIET networks. The involvement of SRB in DIET has been previously documented, where members of this group were shown to directly acquire electrons for sulfate reduction via outer membrane-bound *c*-type cytochromes (Hu et al., 2019; Giangeri et al., 2023). These genera exhibited distinct gene specialization patterns in this study, shedding light on their potential electron transfer strategies.

U*nclassified_f_Desulfovibrionaceae* displayed a clear specialization in e-pili genes abundance, particularly in CFRs. It was the dominant contributor to *pilA* and *pilB*, with CFR-Fe_3O_4 and CFR-PAC showing the highest relative abundance of *pilA*. The genus also contributed moderately to *ccm* genes, though this abundance was largely confined to CFRs, with CFR-Fe_3O_4 and CFR-PAC again showing peak levels. These patterns suggest that *Unclassified_f_Desulfovibrionaceae* functions as a DIET specialist optimized for syntrophic electron transfer via nanowires and cytochromes (Gonzalez et al., 2024). Supporting this, Yang et al. (2024) reported marked enrichment of *Desulfovibrionaceae* in GAC-amended reactors, where they were implicated in syntrophic associations with methanogens, potentially mediated via *pilA*-based DIET mechanisms.

Among the four dominant SRB, *Desulfomicrobium* and *Desulfolutivibrio* exhibited comparable DIET gene abundance patterns, suggesting a shared ecological strategy. Both genera did not express *pilA*, indicating that neither direct-contact nor nanowire-based DIET is their primary electron transfer mode. Instead, they consistently expressed genes related to *ccm* and *rib* genes, implying reliance on cytochrome-dependent and flavin-mediated DIET. *Desulfovibrio* exhibited a flexible but less specialized DIET gene profile, contributing across multiple gene types without clear dominance. In SBR-Fe_3O_4, this genus showed the highest abundance of *pilA*, implying a potential role in e-pili-based electron transfer when Fe_3O_4 was present. Moderate enrichment of *ccm* genes was observed in both SBR and CFR conditions with PAC or Fe_3O_4, indicating support for cytochrome-based DIET in various settings. Zheng et al. (2021) provided direct evidence that *Desulfovibrio* species could donate electrons to methanogens via DIET within conductive methanogenic aggregates. Their metatranscriptomic and coculture studies demonstrated that *Desulfovibrio* expressed abundant cytochrome and e-pili genes and directly transferred electrons to *Methanobacterium* and *Methanothrix*, establishing its capacity for DIET comparable to *Geobacter* in coastal sediments. Additionally, riboflavin synthesis genes were detectable but generally low, suggesting that flavin-mediated electron transfer may serve as an auxiliary mechanism in *Desulfovibrio* (Qian et al., 2023). Collectively, *Desulfovibrio* contributes broadly to multiple DIET mechanisms without strongly favoring any single pathway. Interestingly, *Desulfomicrobium, Desulfolutivibrio*, and *Desulfovibrio* simultaneously dominated in CFRs and expressed the widest array of DIET-related genes. This co-enrichment suggests that continuous operation selectively favors metabolically versatile SRB capable of sustaining multiple electron transfer routes.

In addition to SRB, *Aminivibrio, Pseudomonas*, and *Methanothrix* also exhibited distinct contributions to DIET-related genes. *Aminivibrio* and *Pseudomonas* contributed primarily to *pilB, pilC, ribE*, and *ribF*, with elevated expression in SBRs and moderate abundance in CFRs. Although lacking *ccm* gene abundance, these microorganisms may participate in auxiliary electron transfer processes. *Methanothrix* expressed only the *ribE* gene among all DIET-related genes, with the highest abundance observed in CFR-PAC and CFR-Fe_3O_4. No e-pili- or cytochrome-related genes were detected. The exclusive expression of ribE in *Methanothrix* implies a potential role for flavin-mediated DIET as a complementary electron uptake strategy (Zeng et al., 2024).

3.5. Microbial co-occurrence network analysis

The co-occurrence network analysis provided further insights into microbial interactions within the anaerobic reactors (Fig. 7). The integrated microbial network across the six reactors comprised 50 nodes and 338 edges, with 203 positive correlations outnumbering 135 negative correlations. Positive correlations generally reflect syntrophic interactions or functionally complementary relationships, whereas negative correlations suggest competitive or ecological inhibition (Chen et al., 2021).

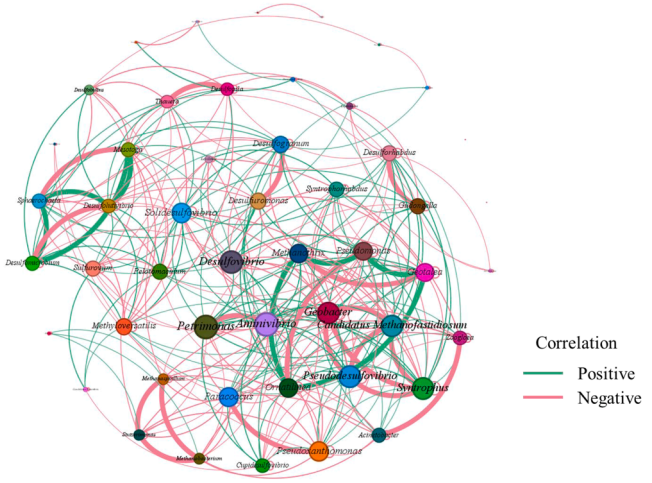

Fig. 7. Microbial co-occurrence network based on genus-level correlations. Node size reflects the average relative abundance of each genus. Green and red edges represent significant positive and negative correlations, respectively.

Several key microbial genera, including *Desulfovibrio, Petrimonas, Aminivibrio, Geobacter, Methanothrix*, and *Syntrophus*, characterized by high connectivity and betweenness centrality, highlighting their pivotal roles in microbial network stability and interspecies electron transfer. *Desulfovibrio*, in particular, exhibited the highest connectivity, reinforcing its inferred role as a versatile DIET participant with broad e-pili, cytochrome and riboflavin biosynthesis gene abundances. Its strong co-occurrence with both SRB (e.g., *Desulfuromonas, Pseudodesulfovibrio*) and methanogens (*Methanothrix*) suggests that it serves as a key conduit in interspecies electron flow. Similar ecological significance has been previously supported by Hu et al. (2019), who demonstrated that *Desulfovibrio* enriched on graphene oxide could modify biocathodes to exhibit highly expressed conductive pili and *c*-type cytochromes, facilitating DIET-linked sulfate reduction. Additionally, Chen et al. (2023a) observed enhanced co-enrichment of *Desulfovibrio* and *Methanosaeta* under GAC-amended anaerobic conditions, implicating *Desulfovibrio* in forming syntrophic DIET-based partnerships with methanogens to improve methanogenesis under sulfide stress. These findings underscore the ecological centrality and functional versatility of *Desulfovibrio* as a key DIET-active microorganism in sulfate-rich anaerobic environments.

Notably, *Geobacter*, although not highly abundant, maintained strong positive correlations with methanogens and several SRB, consistent with its known role as a keystone syntrophic partner in CM-added DIET systems (Zhou et al., 2023).

Moreover, *Methanothrix* exhibited strong positive correlations with a range of syntrophic partners, including SRB (e.g., *Desulfovibrio*, *Desulfuromonas*, and *Cupidesulfovibrio*), fermentative bacteria (e.g., *Syntrophus* and *Syntrophorhabdus*), and canonical electron-donating partners *Geobacter*. These interactions suggest that *Methanothrix* was embedded in a dense syntrophic web facilitating both direct and mediated interspecies electron transfer. Particularly, its co-occurrence with known DIET partners of *Geobacter* and *Desulfovibrio* indicates potential cooperation via CMs or extracellular electron shuttles. In contrast, *Methanothrix* showed negative correlations with genera such as *Pseudomonas*, *Petrimonas*, and *Aminivibrio*, reflecting metabolic competition possibly over substrates like acetate or shared electron donors.

Importantly, *Desulfomicrobium* and *Desulfolutivibrio*, though not ranked as topological hubs in the co-occurrence network, exhibited marked enrichment of cytochrome- and flavin-related DIET genes,

particularly under CFR conditions. Their ecological impact may therefore lie not in broad interspecies connectivity, but in niche-specific electron transfer functions, serving as conditionally important syntrophic partners under CM-facilitated regimes.

4. Conclusion

- This study provides comprehensive comparison of CMs performance under different reactor operational modes of SBR and CFR in sulfate-rich anaerobic systems.
- Reactor configuration fundamentally shaped ethanol metabolism pathways, with SBRs favoring the ethanol-to-propionate pathway via *Desulfobulbus*, while CFRs promoted direct ethanol conversion to acetate.
- CM addition improved sulfate reduction and VFAs turnover, particularly enhancing methane production rate in CFRs.
- At a dosage of 1 g/L, neither Fe_3O_4 nor PAC effectively alleviated H_2S inhibition in SBRs.
- Fe_3O_4 in SBRs primarily functioned as an abiotic conductive conduit that partially replaced the need for microbial conductive structures, whereas, PAC markedly enhanced e-pili and cytochrome gene abundance, especially in CFR-PAC, facilitating cytochrome- and nanowire-based DIET.
- CFRs enriched multiple DIET-active SRB, including *Unclassified_f_Desulfovibrionaceae, Desulfomicrobium, Desulfolutivibrio*, and *Desulfovibrio*, which collectively dominated e-pili, cytochrome, and flavin biosynthesis gene pools.
- Co-occurrence analysis identified *Desulfovibrio, Geobacter*, and *Methanothrix* as key network hubs, with *Desulfovibrio* exhibiting broad interspecies connectivity and functional centrality in CM-enhanced electron transfer.

CRediT authorship contribution statement

Wenhui Shu: Writing – original draft, Methodology, Investigation, Formal analysis. **Guangxue Wu:** Writing – review & editing, Supervision, Methodology, Funding acquisition, Formal analysis, Conceptualization.

Declaration of competing interest

Guangxue Wu reports financial support was provided by Science Foundation Ireland. Guangxue Wu reports financial support was provided by Sustainable Energy Authority of Ireland. Wenhui Shu reports financial support was provided by China Scholarship Council. If there are other authors, they declare that they have no known competing financial interests or personal relationships that could have appeared to influence the work reported in this paper.

Acknowledgements

This study was supported by the Taighde Éireann – Research Ireland (formerly Science Foundation Ireland) and the Sustainable Energy Authority of Ireland under the SFI Frontiers for the Future Awards Programme (22/FFP-A/10346). Wenhui Shu thanks the scholarship from the China Scholarship Council (No: 202106790006). Guangxue Wu thanks for the support from the Galway University Foundation.

Supplementary materials

Supplementary material associated with this article can be found, in the online version, at doi:10.1016/j.watres.2025.124384.

Data availability

Data will be made available on request.

References

APHA, 2005. Standard methods for the examination of water and wastewater, 21st Ed. American Public Health Association, American Water Works Association, Water Environment Federation, Washington DC.
Cavalcante, W.A., Gehring, T.A., Zaiat, M., 2021. Stimulation and inhibition of direct interspecies electron transfer mechanisms within methanogenic reactors by adding magnetite and granular actived carbon. Chem. Eng. J. 415, 128882.
Chen, L., Li, J., Tang, Y., Wang, S., Lu, X., Cheng, Z., Zhang, X., Wu, P., Chang, X., Xia, Y., 2021. Typhoon-induced turbulence redistributed microplastics in coastal areas and reformed plastisphere community. Water Res. 204, 117580.
Chen, L., Zhang, R., Li, Y., Zhang, Y., Fang, W., Zhang, P., Zhang, G., 2023a. Internal driving mechanisms of microbial community and metabolism for granular activated carbon enhancing anaerobic digestion of high-strength sulfate organic wastewater. Chem. Eng. J. 476, 146648.
Chen, L., Zhang, Y., Liang, J., Li, Y., Zhang, J., Fang, W., Zhang, P., Zhang, G., Ngo, H.H., 2023b. Improvement of anaerobic digestion containing sulfur with conductive materials: focusing on recent advances and internal biological mechanisms. Chem. Eng. J. 472, 144867.
Chen, W., Jin, Y., Xu, D., Li, W., Pan, C., Li, Y., Kang, D., Zhang, M., Zeng, Z., Shan, S., Zheng, P., 2022. Underlying function regulators of anaerobic granular sludge: Starvation and dormancy. Sci. Total Environ. 807, 151024.
Cruz Viggi, C., Rossetti, S., Fazi, S., Paiano, P., Majone, M., Aulenta, F., 2014. Magnetite particles triggering a faster and more robust syntrophic pathway of methanogenic propionate degradation. Environ. Sci. Technol. 48 (13), 7536–7543.
Du, B., Zhan, X., Lens, P.N., Zhang, Y., Wu, G., 2024. Deciphering anaerobic ethanol metabolic pathways shaped by operational modes. Water Res 249, 120896.
Du, J., Zhou, X., Yin, Q., Zuo, J., Wu, G., 2023. Revealing impacts of operational modes on anaerobic digestion systems coupling with sulfate reduction. Bioresour. Technol. 385, 129431.
El Houari, A., Ranchou-Peyruse, M., Ranchou-Peyruse, A., Dakdaki, A., Guignard, M., Idouhammou, L., Bennisse, R., Bouterfass, R., Guyoneaud, R., Qatibi, A.I., 2017. *Desulfobulbus oligotrophicus* sp. nov., a sulfate-reducing and propionate-oxidizing bacterium isolated from a municipal anaerobic sewage sludge digester. Int. J. Syst. Evol. Microbiol. 67 (2), 275–281.
Giangeri, G., Tsapekos, P., Gaspari, M., Ghofrani-Isfahani, P., Hong Lin, M.K.T., Treu, L., Kougias, P., Campanaro, S., Angelidaki, I., 2023. Magnetite alters the metabolic interaction between methanogens and sulfate-reducing bacteria. Environ. Sci. Technol. 57 (43), 16399–16413.
Goevert, D., Conrad, R., 2008. Carbon isotope fractionation by sulfate-reducing bacteria using different pathways for the oxidation of acetate. Environ. Sci. Technol. 42 (21), 7813–7817.
Gonzalez, V., Abarca-Hurtado, J., Arancibia, A., Claverías, F., Guevara, M.R., Orellana, R., 2024. Novel insights on extracellular electron transfer networks in the *Desulfovibrionaceae* family: unveiling the potential significance of horizontal gene transfer. Microorganisms 12 (9), 1796.
Hu, J., Zeng, C., Liu, G., Lu, Y., Zhang, R., Luo, H., 2019. Enhanced sulfate reduction accompanied with electrically-conductive pili production in graphene oxide modified biocathodes. Bioresour. Technol. 282, 425–432.
Jin, R.C., Yang, G.F., Zhang, Q.Q., Ma, C., Yu, J.J., Xing, B.S., 2013. The effect of sulfide inhibition on the ANAMMOX process. Water Res 47 (3), 1459–1469.
Jin, Z., Zhao, Z., Zhang, Y., 2019. Potential of direct interspecies electron transfer in synergetic enhancement of methanogenesis and sulfate removal in an up-flow anaerobic sludge blanket reactor with magnetite. Sci. Total Environ. 677, 299–306.
Jung, H., Baek, G., Lee, C., 2020. Magnetite-assisted in situ microbial oxidation of H_2S to S^0 during anaerobic digestion: A new potential for sulfide control. Chem. Eng. J. 397, 124982.
Jung, H., Yu, H., Lee, C., 2023. Direct interspecies electron transfer enables anaerobic oxidation of sulfide to elemental sulfur coupled with CO_2-reducing methanogenesis. iScience 26 (9), 107504.
Kibangou, V.A., Lilly, M., Mpofu, A.B., Jonge, de.N., Oyekola, O.O., Welz, P.J., 2022. Sulfate-reducing and methanogenic microbial community responses during anaerobic digestion of tannery effluent. Bioresour. Technol. 347, 126308.
Lauzurique, Y., Meza, A., Huiliñir, C., Salazar-González, R., Vargas-Morales, G., 2023. Evaluation of the anaerobic digestion of winery wastewater: effect of fly ash in anaerobic sequencing batch reactor. J. Environ. Chem. Eng. 11 (5), 110997.
Lee, S.H., Kang, H.J., Lim, T.G., Park, H.D., 2020. Magnetite and granular activated carbon improve methanogenesis via different metabolic routes. Fuel 281, 118768.
Liang, Z., Ding, W., Zhang, X., Chen, Y., Shen, N., 2025. Magnetite-mediating direct interspecies electron transfer is not pivotal role in directing electrons toward methane production from sulfate containing wastewater. Bioresour. Technol. 416, 131809.
Lien, E., Valsvik, G., Nordstrand, J.V., Martinez, V., Rogne, V., Hafsås, O., Queralt, S., Fathi, B.S., Aga, M., 2022. The SeaRAS AquaSense™ System: Real-time monitoring of H_2S at sub µg/L levels in recirculating aquaculture systems (RAS). Front. Mar. Sci. 9, 894414.
Liu, F., Rotaru, A.E., Shrestha, P.M., Malvankar, N.S., Nevin, K.P., Lovley, D.R., 2015. Magnetite compensates for the lack of a pilin-associated *c*-type cytochrome in extracellular electron exchange. Environ. Microbiol. 17 (3), 648–655.
Liu, Y., Gu, M., Yin, Q., Wu, G., 2019. Inhibition mitigation and ecological mechanism of mesophilic methanogenesis triggered by supplement of ferroferric oxide in sulfate-containing systems. Bioresour. Technol. 288, 121546.
McDonald, M.D., Owusu-Ansah, C., Ellenbogen, J.B., Malone, Z.D., Ricketts, M.P., Frolking, S.E., Ernakovich, J.G., Ibba, M., Bagby, S.C., Weissman, J.L., 2024. What is microbial dormancy? Trends Microbiol 32 (2), 142–150.

O'Flaherty, V., Mahony, T., O'Kennedy, R., Colleran, E., 1998. Effect of pH on growth kinetics and sulphide toxicity thresholds of a range of methanogenic, syntrophic and sulphate-reducing bacteria. Process Biochem 33 (5), 555–569.
Oleszkiewicz, J.A., Marstaller, T., McCartney, D.M., 1989. Effects of pH on sulfide toxicity to anaerobic processes. Environ. Technol. 10 (9), 815–822.
Olivera, C., Tondo, M.L., Girardi, V., Fattobene, L., Herrero, M.S., Pérez, L.M., Salvatierra, L.M., 2022. Early-stage response in anaerobic bioreactors due to high sulfate loads: Hydrogen sulfide yield and other organic volatile sulfur compounds as a sign of microbial community modifications. Bioresour. Technol. 350, 126947.
Oude Elferink, S.J.W.H., Akkermans-van Vliet, W.M., Bogte, J.J., Stams, A.J.M., 1999. *Desulfobacca acetoxidans* gen. nov., sp. nov., a novel acetate-degrading sulfate reducer isolated from sulfidogenic granular sludge. Int. J. Syst. Evol. Microbiol. 49 (2), 345–350.
Paepatung, N., Boonapatcharoen, N., Songkasiri, W., Yasui, H., Phalakornkule, C., 2022. Recovery of anaerobic system treating sulfate-rich wastewater using zero-valent iron. Chem. Eng. J. 435, 135175.
Qian, D., Qi, R., Zhang, S., Chen, Y., Qin, Y., 2023. Interspecific electron transfer-driven oxytetracycline degradation by autotrophic coculture of sulfur-oxidizing and sulfate-reducing bacteria. ACS ES&T Water 3 (4), 1082–1092.
Qiao, W., Takayanagi, K., Li, Q., Shofie, M., Gao, F., Dong, R., Li, Y.Y., 2016. Thermodynamically enhancing propionic acid degradation by using sulfate as an external electron acceptor in a thermophilic anaerobic membrane reactor. Water Res 106, 320–329.
Qian, Z., Tianwei, H., Mackey, H.R., van Loosdrecht, M.C.M., Guanghao, C., 2019. Recent advances in dissimilatory sulfate reduction: from metabolic study to application. Water Res 150, 162–181.
Rombouts, J.L., Mos, G., Weissbrodt, D.G., Kleerebezem, R., Van Loosdrecht, M.C.M., 2019. Diversity and metabolism of xylose and glucose fermenting microbial communities in sequencing batch or continuous culturing. FEMS Microbiol. Ecol. 95 (2), fiy233.
Rotaru, A.E., Shrestha, P.M., Liu, F., Markovaite, B., Chen, S., Nevin, K.P., Lovley, D.R., 2014a. Direct interspecies electron transfer between *Geobacter metallireducens* and *Methanosarcina barkeri*. Appl. Environ. Microbiol. 80 (15), 4599–4605.
Rotaru, A.E., Shrestha, P.M., Liu, F., Shrestha, M., Shrestha, D., Embree, M., Zengler, K., Wardman, C., Nevin, K.P., Lovley, D.R., 2014b. A new model for electron flow during anaerobic digestion: direct interspecies electron transfer to *Methanosaeta* for the reduction of carbon dioxide to methane. Energy Environ. Sci. 7 (1), 408–415.
Shu, W., Du, B., Wu, G., 2025a. Strategies for enriching targeted sulfate-reducing bacteria and revealing their microbial interactions in anaerobic digestion ecosystems. Water Res 270, 122842.
Shu, W., Du, B., Wu, G., 2025b. Deciphering microbial responses to H_2S inhibition of typical functional microorganisms in anaerobic digestion ecosystems. Chem. Eng. J. 513, 162766.
Simon, J., Wiese, J., Steinmetz, H., 2006. A comparison of continuous flow and sequencing batch reactor plants concerning integrated operation of sewer systems and wastewater treatment plants. Water Sci. Technol. 54 (11-12), 241–248.
Stams, A.J.M., Kremer, D.R., Nicolay, K., Weenk, G.H., Hansen, T.A., 1984. Pathway of propionate formation in *Desulfobulbus propionicus*. Arch. Microbiol. 139, 167–173.
Suzuki, D., Ueki, A., Amaishi, A., Ueki, K., 2007. *Desulfobulbus japonicus* sp. nov., a novel Gram-negative propionate-oxidizing, sulfate-reducing bacterium isolated from an estuarine sediment in Japan. Int. J. Syst. Evol. Microbiol. 57 (4), 849–855.
Svetlitchnaia, T., Svetlitchnyi, V., Meyer, O., Dobbek, H., 2006. Structural insights into methyltransfer reactions of a corrinoid iron-sulfur protein involved in acetyl-CoA synthesis. Proc. Natl. Acad. Sci. USA. 103 (39), 14331–14336.
Tong, T., Tong, J., Xue, K., Li, Y., Yu, J., Wei, Y., 2023. Microbial community structure and functional prediction in five full-scale industrial park wastewater treatment plants. Sci. Total Environ. 904, 166529.
Wan, Y.Y., Luo, N., Liu, X.L., Lai, Q.L., Goodfellow, M., 2021. *Cupidesulfovibrio liaohensis* gen. nov., sp. nov., a novel sulphate-reducing bacterium isolated from an oil reservoir and reclassification of *Desulfovibrio oxamicus* and *Desulfovibrio termitidis* as *Cupidesulfovibrio oxamicus* comb. nov. and *Cupidesulfovibrio termitidis* comb. nov. Int. J. Syst. Evol. Microbiol. 71 (2), 004618.
Wang, S., Cheng, S., Zhang, K., Liu, F., Liu, R., Gao, X., Li, J., Du, L., 2024a. Comparing the effects and mechanisms of granular activated carbon and magnetite nanoparticles in dry anaerobic digestion: Focusing on microbial electron transfer and metagenomic evidence. Chem. Eng. J. 497, 155705.
Wang, Y., Fu, Q., Yang, F., Li, X., Ma, X., Xu, Y., Liu, X., Wang, D., 2024b. Mechanistic insights into Fe_3O_4-mediated inhibition of H_2S gas production in sludge anaerobic digestion. Water Res 267, 122464.
Wang, Z., Peng, Y., Li, J., Liu, J., Zhang, Q., Li, X., Zhang, L., 2021. Rapid initiation and stable maintenance of municipal wastewater nitritation during the continuous flow anaerobic/oxic process with an ultra-low sludge retention time. Water Res 197, 117091.
Xie, J., Xu, J., Zhu, J., Zhu, C., He, R., Wang, W., Xie, L., 2022. Roles of Fe-C amendment on sulfate-containing pharmaceutical wastewater anaerobic treatment: Microbial community and sulfur metabolism. Sci. Total Environ. 837, 155868.
Xing, L., Zhang, W., Gu, M., Yin, Q., Wu, G., 2020. Microbial interactions regulated by the dosage of ferroferric oxide in the co-metabolism of organic carbon and sulfate. Bioresour. Technol. 296, 122317.
Xu, C., Ding, Y., Liu, J., Huang, W., Cheng, Q., Fan, G., Yan, J., Zhang, S., Song, G., Xiao, B., 2023. Anaerobic digestion of sulphate wastewater mediated by biochar. Environ. Technol. 44 (11), 1667–1678.
Xu, D., Kang, D., Ding, A., Li, Y., Yu, T., Li, W., Zeng, Z., Guo, L., Zheng, P., 2020. Response of FANIR system to starvation stress: "Dormancy". Water Res 171, 115380.
Xue, J., Yao, Y., Wu, D., Jiang, Q., Shi, K., Gao, Y., Qiao, Y., Wang, B., 2024. Electron Transfer Improved by Nanoscale Zero-Valent Iron to Enhance Sulfate Reduction of the Anaerobic System under a Low Chemical Oxygen Demand-to-Sulfate Ratio. ACS ES&T Water 4 (12), 5608–5620.
Yan, L., Ye, J., Zhang, P., Xu, D., Wu, Y., Liu, J., Zhang, H., Fang, W., Zeng, G., 2018. Hydrogen sulfide formation control and microbial competition in batch anaerobic digestion of slaughterhouse wastewater sludge: Effect of initial sludge pH. Bioresour. Technol. 259, 67–74.
Yang, J., Liu, K., Yi, W., Si, B., Tian, C., Yang, G., 2024. Effects of biochar, granular activated carbon, and magnetite on the electron transfer of microbials during the anaerobic digestion process: insights into nitrogen heterocyclic compounds degradation. Fuel 358, 130079.
Zakaria, B.S., Dhar, B.R., 2022. Intermittent energization catalyzes direct interspecies electron transfer in electro-anaerobic digestion of sewage sludge. Chem. Eng. J. 442, 136177.
Zeng, D., Yin, Q., Du, Q., Wu, G., 2019. System performance and microbial community in ethanol-fed anaerobic reactors acclimated with different organic carbon to sulfate ratios. Bioresour. Technol. 278, 34–42.
Zeng, Y., Liu, H., Chen, W., Li, H., Dong, H., Wu, H., Xu, H., Sun, D., Liu, X., Li, P., Qiu, B., Dang, Y., 2024. Riboflavin-loaded carbon cloth aids the anaerobic digestion of cow dung by promoting direct interspecies electron transfer. Environ. Res. 241, 117660.
Zhang, Q., Yang, Y., Hou, L.A., Zhu, H., Zhang, Y., Pu, J., Li, Y., 2023. Recent advances of carbon-based additives in anaerobic digestion: a review. Renewable Sustainable Energy Rev 183, 113536.
Zhang, S., Ren, Y., Zhao, P., Wang, X., Wang, Q., Sun, X., 2024. Ethanol-type anaerobic digestion enhanced methanogenic performance by stimulating direct interspecies electron transfer and interspecies hydrogen transfer. Bioresour. Technol. 410, 131280.
Zhang, Y., Guo, B., Zhang, L., Zhang, H., Liu, Y., 2021. Microbial community dynamics in granular activated carbon enhanced up-flow anaerobic sludge blanket (UASB) treating municipal sewage under sulfate reducing and psychrophilic conditions. Chem. Eng. J. 405, 126957.
Zhang, Y., Zhang, L., Yu, N., Guo, B., Liu, Y., 2022a. Enhancing the resistance to H_2S toxicity during anaerobic digestion of low-strength wastewater through granular activated carbon (GAC) addition. J. Hazard. Mater. 430, 128473.
Zhang, Z., Zhang, C., Yang, Y., Zhang, Z., Tang, Y., Su, P., Lin, Z., 2022b. A review of sulfate-reducing bacteria: Metabolism, influencing factors and application in wastewater treatment. J. Cleaner Prod. 376, 134109.
Zheng, S., Li, M., Liu, Y., Liu, F., 2021. *Desulfovibrio* feeding *Methanobacterium* with electrons in conductive methanogenic aggregates from coastal zones. Water Res 202, 117490.
Zheng, S., Liu, F., Li, M., Xiao, L., Wang, O., 2018. Comparative transcriptomic insights into the mechanisms of electron transfer in *Geobacter* co-cultures with activated carbon and magnetite. Sci. China: Life Sci 61, 787–798.
Zhou, J., Smith, J.A., Li, M., Holmes, D.E., 2023. Methane production by *Methanothrix thermoacetophila* via direct interspecies electron transfer with *Geobacter metallireducens*. MBio 14 (4), e00360-23.
Zwietering, M.H., Jongenburger, I., Rombouts, F.M., Van't Riet, K., 1990. Modeling of the bacterial growth curve. Appl. Environ. Microbiol. 56 (6), 1875–1881.